Density-functional theory of correlations in dense plasmas: Improvement on the hypernetted-chain scheme

Hiroshi Iyetomi and Setsuo Ichimaru
Department of Physics, University of Tokyo, Bunkyo-ku, Tokyo 113, Japan
(Received 12 November 1982)

Multiparticle correlations in dense plasmas are analyzed in terms of the density-functional formalism; theoretical schemes of improvement over the hypernetted-chain (HNC) approximation are thereby advanced. The proposed schemes contain no adjustable parameters; the computational difficulties associated with these schemes are no greater than those involved in the solution of the ordinary HNC equations. The validity and accuracy of those improved HNC schemes are examined through numerical comparison with the exact Monte Carlo (MC) simulation data; significant improvement over the HNC scheme and close agreement with the MC results are thereby demonstrated.

I. INTRODUCTION

The one-component plasma (OCP) is a classical system of identical point ions with charge Ze, embedded in a rigid, uniform background of neutralizing charges. The thermodynamic state of the OCP with number density n and temperature T is characterized by a single dimensionless parameter Γ defined as

$$\Gamma=\frac{(Ze)^2/a}{k_BT}\ , \tag{1}$$

where a refers to the ion-sphere radius $(\frac{4}{3}\pi n)^{-1/3}$. The OCP system with $\Gamma>1$ provides a physically relevant, nontrivial model to the interior of a heavy planet such as Jupiter, a white dwarf, the outer crust of a neutron star, laser-imploded plasmas, and related substances.[1]

Recently the static properties of such an OCP have been extensively investigated through the Monte Carlo (MC) method by a number of authors[2–4]: Analytical fitting formulas for the internal energy have been provided; the values of the radial distribution function $g(r)$ and the static structure factor $S(q)$ are tabulated for various values of Γ. Difficulties in performing such a direct computer experiment, however, increase tremendously for plasmas near the transition point, or with many ionic species, because of the requirement for increased number of the MC particles which would call for formidable computer time. Therefore, it is not only of physical interest, but also of practical importance, to construct a workable analytic theory for the description of the OCP system whose accuracy is compatible with the MC method.

The hypernetted-chain (HNC) approximation[5] is known to be superior to all of the existing analytic theories for the OCP.[1,6] The HNC approximation, however, still exhibits a systematic departure from the exact MC results in the strong coupling domain ($\Gamma\gg1$): Amplitudes of the oscillations in $g(r)$ are usually underestimated. The HNC form ($\Gamma^{1/2}$) of the "thermal energy" in the internal energy formula differs substantially from the MC form ($\Gamma^{1/4}$) (Ref. 7); these discrepancies are crucial to the calculation of the excess specific heat and the treatment of miscibility[8] in dense, multi-ionic plasmas. Furthermore, the HNC approximation suffers from its internal inconsistency, in that the compressibility sum rule is significantly violated even in the intermediate coupling domain ($\Gamma\simeq1$).

Recently Rosenfeld and Ashcroft[9] have developed a semiempirical scheme of improvement over the HNC approximation, on the basis of the universality ansatz for the bridge function, which is neglected in the HNC approximation. In effect, they assumed the OCP bridge function as given by that of an equivalent hard-sphere reference system, and thereby modified the HNC scheme; their results obtained in this modified scheme turned out to be almost indistinguishable from the MC results. This scheme, however, relies heavily upon the parametrized hard-sphere bridge functions containing the packing fraction η as a free parameter, which is to be determined from a self-consistency condition. Application of this scheme appears increasingly difficult for a multi-ionic plasma, where the number of the free parameters correspondingly increases.

The purpose of the present paper is to develop a

new systematic scheme of improvement on the HNC equation within a self-contained framework of the plasma theory. We present here the theory in terms of the OCP system; however, it is equally applicable to the many-component plasmas as well. In the following section, we formulate the problem using the density-functional method; the bridge function is expressed in terms of the correlation functions. In Sec. III the nature of the HNC approximation is elucidated through the analyses of the correlation functions; we then propose two schemes of improvement over the HNC approximation in Sec. IV. In Sec. V the validity and accuracy of the two schemes are examined through numerical comparison with the exact MC results as well as with the original HNC results; the points of comparison are the radial distribution function, the thermal part of the internal energy, the screening potential, and the compressibility sum rule. Finally, concluding remarks are given in Sec. VI. Some of the mathematical details are described in the Appendices. A preliminary account of the present work has been published elsewhere.[10]

II. DENSITY-FUNCTIONAL FORMALISM

According to the density-functional formalism,[11] the free energy of an inhomogeneous OCP in the presence of a static external field $\phi_{\rm ext}(\vec{r})$ is written in terms of functionals of density deviation $\delta n(\vec{r})=n(\vec{r})-n$ as

$$F[n(\vec{r})]=F_0[n(\vec{r})]+\frac{1}{2}\int v(|\vec{r}-\vec{r}'|)\delta n(\vec{r})\delta n(\vec{r}')d\vec{r}\,d\vec{r}'+F_c[n(\vec{r})]+Ze\int \delta n(\vec{r})\phi_{\rm ext}(\vec{r})d\vec{r}\,. \tag{2}$$

Here $v(r)$ is the Coulomb potential $(Ze)^2/r$, $F_0[n(\vec{r})]$ denotes the free-energy functional of the corresponding noninteracting system, and $F_c[n(\vec{r})]$ represents the remaining free-energy contribution due to correlational effects. The density distribution in thermodynamic equilibrium is determined by minimizing $F[n(\vec{r})]$ with respect to $\delta n(\vec{r})$.[11]

For later convenience we expand $F_c[n(\vec{r})]$ around the homogeneous density n as

$$F_c[n(\vec{r})]=F_c[n]+\frac{1}{2!}\int K_c^{(2)}(|\vec{r}-\vec{r}'|)\delta n(\vec{r})\delta n(\vec{r}')d\vec{r}\,d\vec{r}' +\frac{1}{3!}\int K_c^{(3)}(\vec{r}-\vec{r}',\vec{r}-\vec{r}'')\delta n(\vec{r})\delta n(\vec{r}')\delta n(\vec{r}'')d\vec{r}\,d\vec{r}'\,d\vec{r}''+\cdots\,, \tag{3}$$

where the first-order term vanishes by virtue of particle-number conservation. The integral kernel $K_c^{(\nu)}(\vec{r}_1,\ldots,\vec{r}_\nu)$ physically describes the ν-body interaction among the induced density deviations arising from the particle correlations.

The ν-body correlation potential $K_c^{(\nu)}(\vec{r}_1,\ldots,\vec{r}_\nu)$ can be calculated by means of the functional derivative method[12]; the results for the Fourier transforms of $K_c^{(2)}(\vec{r}_1,\vec{r}_2)$ and $K_c^{(3)}(\vec{r}_1,\vec{r}_2,\vec{r}_3)$ are

$$\beta\tilde{K}_c^{(2)}(q)=-\beta\tilde{v}(q)-\tilde{c}(q)\,, \tag{4}$$

$$n^2\beta\tilde{K}_c^{(3)}(\vec{p},\vec{q})=1-S^{(3)}(\vec{p},\vec{q})/S(p)S(q)S(k)\,, \tag{5}$$

where $\beta=(k_BT)^{-1}$, $\tilde{v}(q)=4\pi(Ze)^2/q^2$, and $\vec{k}=\vec{p}+\vec{q}$. The functions $S(q)$ and $\tilde{c}(q)$ are the static structure factor and the Fourier transform of the direct correlation function $c(r)$, connected to each other via the Ornstein-Zernike relation:

$$\tilde{c}(q)=\frac{1}{n}\left[1-\frac{1}{S(q)}\right]. \tag{6}$$

The function $S^{(3)}(\vec{p},\vec{q})$ is a three-body analog of $S(q)$, expressed in terms of the Fourier transform of the ternary correlation function $h^{(3)}(\vec{r}_1,\vec{r}_2,\vec{r}_3)$ as

$$S^{(3)}(\vec{p},\vec{q})=-2+S(p)+S(q)+S(k)+n^2\tilde{h}^{(3)}(\vec{p},\vec{q})\,. \tag{7}$$

The explicit expression for $\tilde{K}_c^{(4)}(\vec{q}_1,\vec{q}_2,\vec{q}_3)$ in terms of the correlation functions is given in Appendix A.

If a test particle identical to a plasma particle is introduced at the origin, that is, if we set $\phi_{\rm ext}(\vec{r})=Ze/r$, the relative density $n(\vec{r})/n$ would amount to the radial distribution function $g(r)$. We thus find an exact equation for $g(r)$,

$$g(r)=\exp[-\beta v(r)+h(r)-c(r)+B(r)]\,, \tag{8}$$

where we take note of the Ornstein-Zernike relation between the direct correlation function $c(r)$ and the pair correlation function, $h(r)=g(r)-1$:

$$h(r)=c(r)+n\int h(|\vec{r}-\vec{r}'|)c(r')d\vec{r}'\,. \tag{9}$$

The function $B(r)$ in the density-functional theory is given by

$$B(r)=-\frac{\beta n^2}{2!}\int K_c^{(3)}(\vec{r}-\vec{r}',\vec{r}-\vec{r}'')h(r')h(r'')d\vec{r}'d\vec{r}''$$
$$-\frac{\beta n^3}{3!}\int K_c^{(4)}(\vec{r}-\vec{r}',\vec{r}-\vec{r}'',\vec{r}-\vec{r}''')h(r')h(r'')h(r''')d\vec{r}'d\vec{r}''d\vec{r}'''-\cdots , \quad (10)$$

which corresponds to the sum of all the bridge diagrams in the Mayer cluster expansion; this equation therefore provides an essential link between the diagrammatic expansion theory and the density-functional formalism.[13]

The HNC equation is obtained if one sets $B(r)=0$ in (8). Hence the improvement of the HNC approximation may be achieved through evaluation of the bridge function $B(r)$, which may be done by taking account of the three-body and higher-order density correlations on the basis of the Eq. (10).

III. CORRELATIONAL EFFECTS IN THE BRIDGE FUNCTION

Let us now investigate how the various correlation functions are involved in the evaluation of the bridge function through the expansion (10).

In so doing we first note that the static structure factor for the OCP vanishes in the long-wavelength limit according to

$$S(q)\rightarrow\frac{k_BT}{4\pi n(Ze)^2}q^2, \text{ as } q\rightarrow 0 . \quad (11)$$

In the light of (6), we then find that the two-particle correlation potential (4) converges in this limit, since the divergent Coulomb-interaction term $\beta\tilde{v}(q)$ cancels with an analogous, divergent term arising from $\tilde{c}(q)$; $K_c^{(2)}(q)$ thus represents a short-range potential.

We are now concerned with the question of whether or not the higher-order correlation potentials, $K_c^{(\nu)}(\vec{r}_1,\ldots,\vec{r}_\nu)$ with $\nu\geq 3$, are likewise short-range ones; those potentials are directly involved in the evaluation of the bridge function (10). As we observe in (5), $\tilde{K}_c^{(3)}(\vec{p},\vec{q})$ would seem to diverge in the long-wavelength domain because of the product of structure factors in its denominator; $\tilde{K}_c^{(\nu)}(\vec{q}_1,..,\vec{q}_\nu)$ where $\vec{q}_1+\cdots+\vec{q}_\nu=0$ $(\nu\geq 4)$ would exhibit even stronger divergence as Eq. (A1) exemplifies.

It is possible to prove, however, that all the higher-order correlation potentials are in fact short-range ones. The proof follows directly from the sequential relations between the many-particle correlation functions:

$$\int h^{(\nu+1)}(\vec{r}_1,\ldots,\vec{r}_{\nu+1})d\vec{r}_{\nu+1}$$
$$=-\frac{\nu}{n}h^{(\nu)}(\vec{r}_1,\ldots,\vec{r}_\nu) , \quad (12)$$

with $h^{(2)}(\vec{r}_1,\vec{r}_2)=h(r_{12})$, $r_{12}=|\vec{r}_1-\vec{r}_2|$, and

$$\int h(r)d\vec{r}=-\frac{1}{n} . \quad (13)$$

The relations (12) and (13) stem from the conservation of number of the particles in the definition of the correlation functions. That $\tilde{K}_c^{(3)}(\vec{p},\vec{q})$ actually represents a nondivergent, short-range potential has been proved from (12) at $\nu=3$ by Chakravarty and Ashcroft.[14] A general proof on $\tilde{K}_c^{(\nu)}(\vec{q}_1,\ldots,\vec{q}_\nu)$ with $\nu\geq 4$ is lengthy and will be published separately.[15]

Since all the correlation potentials are short ranged, it follows from (10) that the bridge function itself is likewise short ranged. A similar conclusion has been reached by Deutsch, Furutani, and Gombert,[16] though in quite a different context, through the method of nodal expansion.

The correlation functions expressed in the convolution approximation (CA) (Ref. 17) satisfy the sequential relations (12) exactly. The ternary-correlation function in CA reads

$$h_{\rm CA}^{(3)}(\vec{r}_1,\vec{r}_2,\vec{r}_3)=h(r_{12})h(r_{13})+h(r_{12})h(r_{23})$$
$$+h(r_{13})h(r_{23})$$
$$+n\int h(r_{14})h(r_{24})h(r_{34})d\vec{r}_4 . \quad (14)$$

On substituting (14) in (5) with the aid of (7) and (13), one finds $\tilde{K}_c^{(3)}(\vec{p},\vec{q})=0$ in CA. It is in fact possible to show[15] that all the higher-order correlation potentials vanish identically in the convolution approximation. Hence, we find that the adoption of the convolution approximation directly leads to $B(r)=0$ or the HNC equation. This observation elucidates the reason why the HNC scheme has been so successful in describing the correlational properties for the Coulomb systems; the convolution approximation, satisfying (12), takes accurate account of the long-range correlations, which are crucial in a Coulomb system. The HNC scheme is less accurate in the short-range domain since it neglects the bridge function, which is short ranged even in a Coulomb system.

IV. IMPROVED HNC SCHEMES

We have noted that the convolution approximation on which the HNC scheme is based takes a

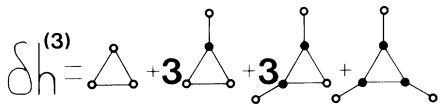

FIG. 1. Kirkwood superposition-approximation terms with vertex corrections. Open circles refer to the particle coordinates under consideration; the filled circles, those to be integrated with number density n; and a line joining two particles represents the correlation function $h(r)$.

good account of the long-range correlations and that the bridge function which is neglected in the HNC approximation represents basically a short-range effect. To find a theoretical scheme by which the HNC equation is systematically improved, therefore, one must pay special attention to the correlations in the short-range domain.

We thus single out the CA contribution in the ternary-correlation function and write

$$h^{(3)}(\vec{r}_1,\vec{r}_2,\vec{r}_3)=h^{(3)}_{\mathrm{CA}}(\vec{r}_1,\vec{r}_2,\vec{r}_3) +\delta h^{(3)}(\vec{r}_1,\vec{r}_2,\vec{r}_3)\ , \tag{15}$$

where we take $\delta h^{(3)}(\vec{r}_1,\vec{r}_2,\vec{r}_3)$ to represent especially the short-range correlation effect. The Kirkwood superposition-approximation term, given by the first, triangular term in Fig. 1, may offer a simplest term describing such an effect. The sequential relations (12) being violated, however, the use of this term alone in (15) would lead to a spurious divergence in $\tilde{K}_c^{(3)}(\vec{p},\vec{q})$. To rectify this apparent flaw, we convolute each vertex and collect all the diagrams as depicted in Fig. 1; the result is

$$\beta K^{(3)}_{\mathrm{CK}}(\vec{r}_1,\vec{r}_2,\vec{r}_3)=-h(r_{12})h(r_{23})h(r_{31})\ . \tag{16}$$

Substitution of (16) in (10) yields a contribution to the bridge function,

$$B_{\mathrm{CK}}(r) =\frac{n^2}{2}\int d\vec{r}'\int d\vec{r}''h(|\vec{r}-\vec{r}'|)h(|\vec{r}'-\vec{r}''|) \times h(|\vec{r}''-\vec{r}|)h(r')h(r'')\ . \tag{17}$$

The ternary contribution $B_{\mathrm{CK}}(r)$ obtained above turns out to be the simplest bridge-diagram contribution where the h bond replaces the Debye bond in the nodal expansion. The density-functional method used in the derivation of (17) clearly illustrates its physical origin.

In order to clarify the picture and to simplify the treatment, we evaluate $B_{\mathrm{CK}}(r)$ numerically by substituting the HNC values $h_H(r)$ in place of $h(r)$ in (17). In Fig. 2, we plot the resultant values of $B_{\mathrm{CK}}(r)$ as a function of reduced distance r/a for various Γ. The numerical details in the calculation of $B_{\mathrm{CK}}(r)$ are described in Appendix B.

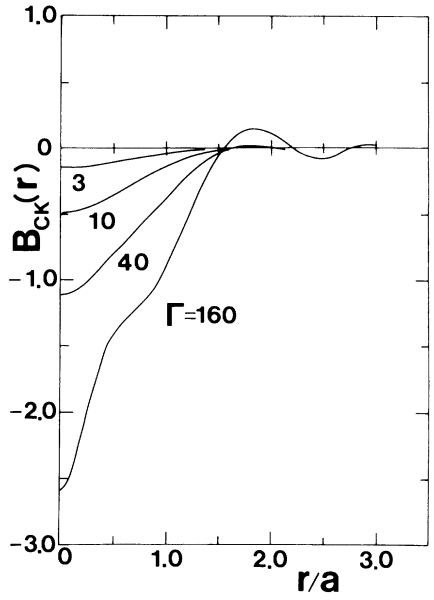

FIG. 2. Ternary-correlation contribution $B_{\mathrm{CK}}(r)$ for various values of Γ, calculated according to Eq. (17) with $h_H(r)$ in place of $h(r)$.

The ternary-correlation contribution $B_{\mathrm{CK}}(r)$ to the bridge function acts in effect as a repulsive short-range potential, modifying the HNC effective potential via Eq. (8). This corroborates the observation advanced by Rosenfeld and Ashcroft[9] on the role of the bridge function. As Γ increases, the repulsive potential of $B_{\mathrm{CK}}(r)$ deepens; in addition, for $\Gamma \geq 40$, an attractive part of $B_{\mathrm{CK}}(r)$ begins to appear in the vicinity of the first peak of $g(r)$. Such an attractive part of $B_{\mathrm{CK}}(r)$ has not been taken into consideration in the parametrized bridge function of Rosenfeld and Ashcroft. The functional behavior of $B_{\mathrm{CK}}(r)$ computed through Eq. (17) thus contains those elements desirable for the necessary improvement on the HNC equation; inclusion of $B_{\mathrm{CK}}(r)$ in (8) tends to enhance the oscillations of $g(r)$, which have been underestimated in the HNC approximation.

We now proceed to investigate the four-particle and higher-order correlation contributions in the evaluation of the bridge function $B(r)$. Although the higher-order correlations are expected to decay much more rapidly than the ternary correlation at

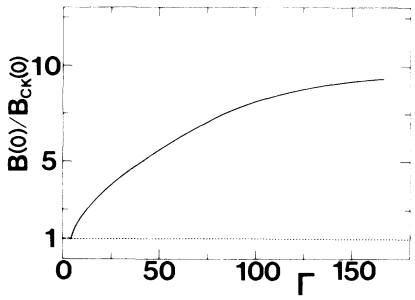

FIG. 3. Ratio of $B(0)$ to $B_{\mathrm{CK}}(0)$ as a function of Γ.

long distances, they may have dominant influences on the behavior of $B(r)$ near the origin, $r \simeq 0$. A reliable estimate on the value of $B(r)$ at the origin would, therefore, provide a measure of the extent to which the higher-order correlational effects are involved in the bridge function through a comparison between $B_{\mathrm{CK}}(0)$ and $B(0)$.

For this purpose we estimate $B(0)$ as follows: The bridge function $B(r)$ is expressed in terms of the screening potential $H(r)$ as[1]

$$B(r)=H(r)+c(r)-h(r) . \tag{18}$$

The values of $H(0)$ may be obtained with the ion-sphere (IS) model,[1,18] valid in the strong coupling domain ($\Gamma \gg 1$), as

$$H_{\mathrm{IS}}(0)=1.057\Gamma . \tag{19}$$

For $c(0)$ we use the HNC values $c_H(r)$, which for $\Gamma \geq 50$ is expressed as

$$c_H(0)=-1.22\Gamma . \tag{20}$$

These estimates differ slightly from the exact MC values, but are sufficiently accurate for the present purposes. Finally, we note

$$h(0)=-1 , \tag{21}$$

by virtue of $g(0)=0$ for a classical OCP. Substitution of those values in Eq. (18) yields our heuristic estimates for $B(0)$, which for $\Gamma \gg 1$ may approach

$$B(0)=-0.16\Gamma+1 . \tag{22}$$

In Fig. 3 we plot the ratio $B(0)/B_{\mathrm{CK}}(0)$ as a function of Γ. In the intermediate coupling domain ($\Gamma \simeq 1$), the higher-order contributions are negligible as compared with the ternary-correlation contribution [i.e., $B(0)/B_{\mathrm{CK}}(0) \simeq 1$].[19] The importance of those higher-order effects increases monotonically with Γ, however; consideration of the ternary contribution $B_{\mathrm{CK}}(r)$ alone becomes insufficient in the large Γ domain.

In principle, one can systematically improve the approximation for $B(r)$ by taking into account the contribution of those diagrams of higher order than (17) through (10). A numerical computation of such a higher-order diagram naturally calls for multidimensional integrations of increased complexity, whose accurate evaluations would be a task of formidable difficulty. Even if such a computation should turn out feasible for a few extra diagrams, our point of view is that such a perturbation-theoretical treatment may not yield fruitful results for a strongly coupled plasma with $\Gamma \gg 1$.

Instead here we attempt to renormalize the short-range part of $B_{\mathrm{CK}}(r)$ by introducing a function $f(r)$ in a form as

$$B(r)=f(r)B_{\mathrm{CK}}(r) . \tag{23}$$

The stretching function $f(r)$ takes on the value $B(0)/B_{\mathrm{CK}}(0)$ at the origin and is expected to approach unity as r increases with a characteristic decay length ξ arising from the decreased degrees of contributions from the four-body and higher-order density correlations. This renormalization procedure should physically correspond to resummation of all the higher-order bridge diagrams according to the ion-sphere model.

The simplest choice for $f(r)$ is to set

$$f(r)=B(0)/B_{\mathrm{CK}}(0) , \tag{24}$$

which neglects the decaying behavior of $f(r)$ at large distances. Since $B_{\mathrm{CK}}(r)$ is already a short-ranged function, one expects that inherent inaccuracies in the treatment of the long-range part according to (24) may not be substantial. For brevity this approximation will be hereafter called scheme I. This scheme is analogous, in principle, to what has been recently studied as HNC/S by Usmani, Friedman, and Pandharipande.[20]

To materialize the decaying behavior of $f(r)$ for the long distances, we may alternatively adopt the form,

$$f(r)=\left[\frac{B(0)}{B_{\mathrm{CK}}(0)}-1\right]\exp\left[-\left[\frac{r}{\xi a}\right]^2\right]+1 , \tag{25}$$

where we set $\xi=1.6$ reflecting the distance at which $B_{\mathrm{CK}}(r)$ vanishes for the first time. Although there remains a small room of adjustment in this determination of ξ, we shall show in the following section that the final numerical results are rather insensitive to such a freedom. The approximation according to (25) will be referred to as scheme II.

As the bridge function is evaluated according to

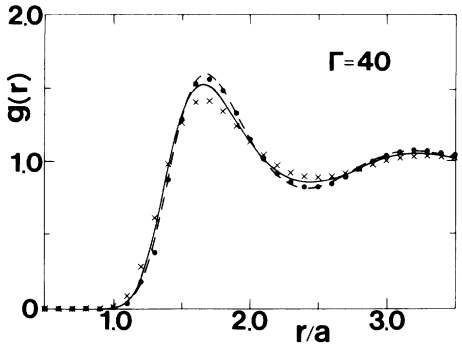

FIG. 4. Radial distribution function $g(r)$ for OCP at $\Gamma=40$. Filled circles represent the MC values taken from Ref. 2; the crosses, the HNC values. Dashed and solid curves depict the IHNC values of $g(r)$ in schemes I and II, respectively.

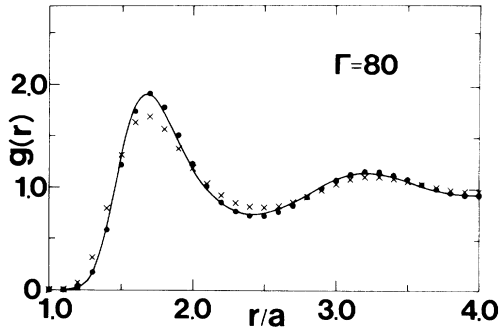

FIG. 5. Radial distribution function $g(r)$ for OCP at $\Gamma=80$. Filled circles represent the MC values taken from Ref. 4; the crosses, the HNC values. Solid curve depicts the IHNC values of $g(r)$ in scheme II.

(23), either with (24) or with (25), it is now a straightforward task to provide a scheme of improvement over the HNC equation: In the light of the exact equation (8), we may take

$$v_{\text{eff}}(r)=v(r)-B(r)/\beta\ , \tag{26}$$

and regard it as the effective potential, to be used in the HNC equation. Combining this modified HNC equation with the Ornstein-Zernike relation, we have a closed, self-consistent scheme by which various correlation functions are determined.

V. NUMERICAL RESULTS AND DISCUSSION

In this section we present the numerical results for the solution to the improved hypernetted-chain (IHNC) equation with the bridge function as evaluated according to schemes I and II. For the details of the computational method in the solution to the HNC equation, we refer the reader to Ng (Ref. 21); our results obtained in the simple HNC scheme agree completely with those of Ng, ensuring reliability of the computational procedures.

In Fig. 4, we show the IHNC values of $g(r)$ for $\Gamma=40$, together with the HNC and MC values. Scheme I reproduces the MC data almost identically. Scheme II likewise improves significantly over the HNC results, although it does not agree with the MC data as closely as scheme I. As Γ increases beyond $\Gamma=40$, however, scheme I breaks down; the use of the stretching factor, Eq. (24), acts to overemphasize the long-range attractive part of the bridge function beyond the first-peak position of $g(r)$, resulting in overenhancement of the oscillation in $g(r)$ as compared with the MC results. As we have noted earlier, the simplest bridge-diagram contribution $B_{\text{CK}}(r)$ already takes account of the major part of the corrections to the HNC approximation in the long-range domain; no stretching of $B_{\text{CK}}(r)$ is essentially needed there.

In Figs. 5 and 6, we thus present the IHNC results of $g(r)$ calculated only in scheme II at $\Gamma=80$ and 160, and compare them with the HNC and MC results. We see here that IHNC values agree very well with the corresponding MC data. The IHNC static structure factor $S(q)$ in scheme II at $\Gamma=100$ is also shown in Fig. 7. Here again, the agreement with the MC results is excellent.

The IHNC solutions obtained in scheme II are actually quite insensitive to the choice of the characteristic decay length ξ. In Table I we illustrate this insensitivity by listing the values of the first peak in $g(r)$ computed with $\xi=1.5$, 1.6, and 1.7 at $\Gamma=80$ and 160, together with the HNC and MC values.

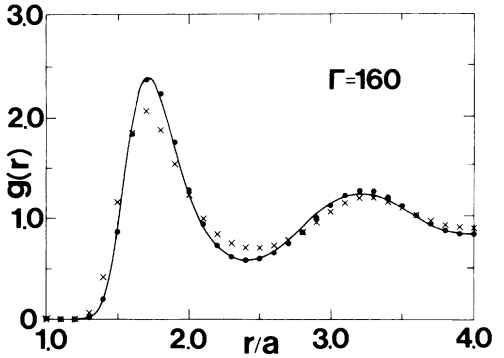

FIG. 6. Same as Fig. 5, at $\Gamma=160$.

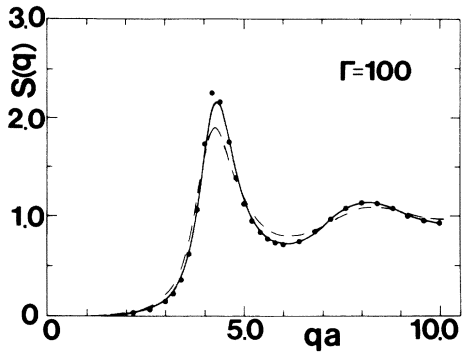

FIG. 7. OCP static structure factor $S(q)$ at $\Gamma=100$. Dashed curve represents the HNC values of $S(q)$; the solid curve represents the IHNC values obtained in scheme II. Filled circles are the MC data taken from Ref. 22.

The largest relative variation of the first-peak values due to the change of ξ from 1.5 to 1.7 is 2% at $\Gamma=160$. The observation that the results are numerically insensitive to ξ eliminates an element of arbitrariness in scheme II.

Next, we investigate the thermal part u_T of the excess internal energy u_e. The thermal part u_T may be defined[7] as the difference between u_e and the Madelung energy $-0.895\,93\Gamma$ of the body-centered-cubic (bcc) Coulomb lattice, that is,

$$u_T=u_e+0.895\,93\Gamma\ . \tag{27}$$

The functional dependence of u_T on Γ, thus, characterizes the fluid nature of the OCP. Table II compares the IHNC values of u_T based upon schemes I and II with the HNC and MC values. Since scheme I breaks down beyond $\Gamma=40$, the values calculated in scheme I are not listed for $\Gamma>40$. Since the IHNC scheme incorporates the bridge-diagram contributions, the functional behavior of u_T deviates from the HNC form ($\Gamma^{1/2}$) and approaches close to the MC form ($\Gamma^{1/4}$). In particular, the IHNC values in scheme I are almost identical to the MC counterparts for $\Gamma\leq 40$. Here again the insensitivity to the choice of ξ is reconfirmed by noting that the relative variation of the excess internal energy due to a change of ξ from 1.5 and 1.7 is less than 0.1% at $\Gamma=160$.

TABLE I. First peak values of the radial distribution function $g(r)$. The MC values are taken from Ref. 4.

			IHNC(II)		
Γ	HNC	MC	$\xi=1.5$	1.6	1.7
80	1.69	1.91	1.89	1.91	1.92
160	2.06	2.38	2.38	2.41	2.43

TABLE II. Thermal fraction u_T of the excess internal energy calculated in various schemes. The MC results are taken from Ref. 4.

Γ	HNC	MC	IHNC (I)	IHNC (II)
3	0.585	0.575	0.577	
6	0.814	0.784	0.790	0.792
10	1.02	0.97	0.98	
20	1.38	1.25	1.28	1.30
40	1.84	1.58	1.59	1.68
80	2.41	1.96		2.10
125	2.84	2.21		2.39
160	3.09	2.36		2.56

The screening potential $H(r)$ for the OCP plays an important role in the calculation of enhancement of thermonuclear reaction rate in the dense stellar plasmas.[23–25] Figure 8 illustrates comparison of the IHNC values of $H(r)$ in scheme II with the HNC and MC results at $\Gamma=80$ and 160. The dashed lines represent the fitting formula[24] proposed for the MC simulation data,

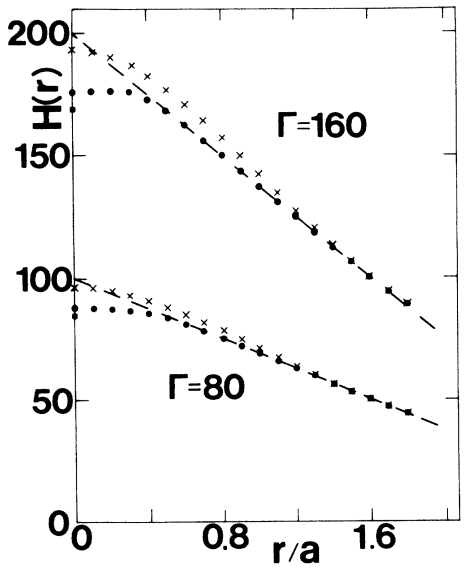

FIG. 8. OCP screening potential $H(r)$ for $\Gamma=80$ and 160. Dashed line refers to the MC fit given by Eq. (28). Crosses represent the HNC values; the filled circles represent the IHNC values in scheme II. Squares represent the ion-sphere result $H_{IS}(0)$, Eq. (19).

TABLE III. The isothermal compressibility computed in various schemes. The column MC lists the inverse isothermal compressibility $\beta/n\kappa_T$ calculated from the MC equation of state (Ref. 4); HNC, $\beta/n\kappa_T$ calculated from the long-wavelength limit of the HNC values of $S(q)$; IHNC (I) and IHNC (II), $\beta/n\kappa_T$ from the long-wavelength limit of the IHNC values of $S(q)$ in schemes I and II, respectively.

Γ	MC	HNC	IHNC (I)	IHNC (II)
3	0.028	−0.088	−0.005	
6	−1.09	−1.46	−1.19	−1.23
10	−2.62	−3.42	−2.84	
20	−6.50	−8.63	−7.35	−7.77
40	−14.34	−19.55	−17.14	−18.15
80	−30.14	−42.19		−40.53
125	−47.97	−68.19		−66.61
160	−61.86	−88.62		−87.03

$$H(r)=\Gamma[1.25-0.39(r/a)] \quad (0.4\lesssim r/a\lesssim 1.8)\ . \tag{28}$$

As we observe in Fig. 8, the IHNC results reproduce this linear behavior of $H(r)$ in the range of $0.4\lesssim r/a\lesssim 1.8$ In addition, the convex behavior of the IHNC values near the origin are compatible with the exact small r expansion[25] of $H(r)$, i.e.,

$$H(r)=H(0)-\frac{\Gamma}{4}\left[\frac{r}{a}\right]^2+\cdots\ . \tag{29}$$

Finally, we examine the extent to which the compressibility sum rule[1] is satisfied in the present IHNC schemes, as compared with the HNC approximation. In Table III, the isothermal compressibility κ_T, calculated in two different ways, namely, from the equation of state and from the long-wavelength limit of $S(q)$, is listed for various Γ. Since the compressibilities obtained by differentiating the equation of state are indistinguishable among the HNC, MC, and IHNC schemes, agreeing with each other within 1%, only the MC results are listed here. The compressibility determined from the long-wavelength limit of $S(q)$ is calculated through the relation[6]

$$\beta/n\kappa_T=1-\lim_{q\to 0}\{n\tilde{c}(q)+[4\pi n(Ze)^2/k_BTq^2]\}\ . \tag{30}$$

Schemes I and II substantially improve over the HNC results in the range of $\Gamma\lesssim 40$. Scheme II, however, does not seem to improve significantly on the internal inconsistency observed in the HNC compressibilities for $\Gamma\gtrsim 40$; the IHNC results are only slightly shifted toward the MC counterparts. This lack of improvement on the compressibility sum rule may have resulted from the slight disagreement between the IHNC and MC values of $c(r)$; for instance, the IHNC value of $c(0)$ (Ref. 26) in scheme II behaves as -1.26Γ for $\Gamma\gtrsim 40$, contrary to the exact MC results,[6] -1.33Γ. It may require a different choice of the functional form of $f(r)$ to achieve a complete agreement in the compressibility sum rule.

VI. CONCLUDING REMARKS

We have presented two theoretical schemes by which the HNC approximation is systematically improved for the OCP. Scheme I depends on the evaluation of the bridge function according to Eqs. (17) and (18), while scheme II uses a different choice of the stretching function Eq. (19) together with Eq. (17). On the basis of those evaluations, the improved HNC schemes have been advanced for the calculation of correlations in dense plasmas. The proposed schemes contain no free parameters; the computational difficulties associated with these schemes are no greater than those involved in the solution of the ordinary HNC equation. The schemes can easily be extended to the cases of multicomponent plasmas.

The validity and accuracy of those improved HNC schemes have been examined through numerical comparison with the exact MC data. Scheme I reproduces the MC results almost perfectly, although its range of applicability is limited to $\Gamma\lesssim 40$. Scheme II, on the other hand, is applicable with good accuracy for all the parameter domain of the plasma fluid and improves significantly over the HNC results.

ACKNOWLEDGMENTS

This work was supported in part by the Japanese Ministry of Education, Science, and Culture through Research Grants 56380001 and 57340023.

APPENDIX A: EXPRESSION OF $\tilde{K}_c^{(4)}(\vec{q}_1,\vec{q}_2,\vec{q}_3)$ IN TERMS OF THE CORRELATION FUNCTIONS

The result for $\tilde{K}_c^{(4)}(\vec{q}_1,\vec{q}_2,\vec{q}_3)$ is

$$n^3\beta\tilde{K}_c^{(4)}(\vec{q}_1,\vec{q}_2,\vec{q}_3)=-2-\frac{S^{(4)}(\vec{q}_1,\vec{q}_2,\vec{q}_3)}{S(q_1)S(q_2)S(q_3)S(q_4)}+\left[\frac{S^{(3)}(\vec{q}_1,\vec{q}_2)S^{(3)}(\vec{q}_1+\vec{q}_2,\vec{q}_3)}{S(q_1)S(q_2)S(q_3)S(q_4)S(|\vec{q}_1+\vec{q}_2|)}+(\cdots)\right], \tag{A1}$$

where $\vec{q}_4=\vec{q}_1+\vec{q}_2+\vec{q}_3$, and $(\cdots)$ denotes those terms arising from cyclic permutations of $\vec{q}_1$, $\vec{q}_2$, and $\vec{q}_3$ in the first term. The function $S^{(4)}(\vec{q}_1,\vec{q}_2,\vec{q}_3)$ is expressed in terms of the Fourier transform of the correlation functions as

$$S^{(4)}(\vec{q}_1,\vec{q}_2,\vec{q}_3)=1+n\{\tilde{h}(q_1)+\tilde{h}(q_2)+\tilde{h}(q_3)+\tilde{h}(q_4)+\tilde{h}(|\vec{q}_1+\vec{q}_2|)+\tilde{h}(|\vec{q}_2+\vec{q}_3|)+\tilde{h}(|\vec{q}_3+\vec{q}_1|)\}$$
$$+n^2\{\tilde{h}^{(3)}(\vec{q}_1,\vec{q}_2)+\tilde{h}^{(3)}(\vec{q}_2,\vec{q}_3)+\tilde{h}^{(3)}(\vec{q}_3,\vec{q}_1)+\tilde{h}^{(3)}(\vec{q}_1,\vec{q}_2+\vec{q}_3)+\tilde{h}^{(3)}(\vec{q}_2,\vec{q}_3+\vec{q}_1)$$
$$+\tilde{h}^{(3)}(\vec{q}_3,\vec{q}_1+\vec{q}_2)\}+n^3\tilde{h}^{(4)}(\vec{q}_1,\vec{q}_2,\vec{q}_3)\ , \tag{A2}$$

where the function $\tilde{h}^{(4)}(\vec{q}_1,\vec{q}_2,\vec{q}_3)$ denotes the Fourier transform of the usual quaternary-correlation function $h^{(4)}(\vec{r}_1,\vec{r}_2,\vec{r}_3,\vec{r}_4)$.[27]

APPENDIX B: SCHEME OF NUMERICAL INTEGRATIONS IN $B_{CK}(r)$

In order to obtain the numerical accuracy in the integration of $B_{CK}(r)$ we expand $h_H(r)$ in the Legendre polynomials as

$$h_H(|\vec{r}-\vec{r}'|)=\sum_{l=0}^{\infty}A_l(r,r')P_l(\cos\theta)\ , \tag{B1}$$

where $\cos\theta$ is the direction cosine between $\vec{r}$ and $\vec{r}'$. The function $A_l(r,r')$ is given by

$$A_l(r,r')=(\tfrac{1}{2}+l)\int_{-1}^{1}h_H(|\vec{r}-\vec{r}'|)P_l(\cos\theta)d(\cos\theta)\ . \tag{B2}$$

Substituting Eq. (B2) in Eq. (17), one can explicitly carry out the direction integrals with the aid of the addition theorem for the spherical harmonics. Finally, one obtains the following tractable expression for $B_{CK}(r)$, reduced to double integrations with respect to r' and r'' only:

$$B_{CK}(r)=8\pi^2n^2\sum_{l=0}^{\infty}\frac{1}{(2l+1)^2}\int_0^{\infty}dr'\int_0^{\infty}dr''(r')^2(r'')^2A_l(r,r')A_l(r'r'')A_l(r'',r)h_H(r')h_H(r'')\ . \tag{B3}$$

Since Eq. (B3) is in a form of series expansion, it may be easy to check its convergence numerically. In the present calculations we have taken the first ten terms in this series expansion. The above technique, which is useful in computing the multiple integrations, was originally used in the calculation of the virial coefficients by Barker and Monaghan.[28]

[1] S. Ichimaru, Rev. Mod. Phys. 54, 1017 (1982).

[2] S. G. Brush, H. L. Sahlin, and E. Teller, J. Chem. Phys. 45, 2102 (1966).

[3] J. P. Hansen, Phys. Rev. A 8, 3096 (1973).

[4] W. L. Slattery, G. D. Doolen, and H. E. DeWitt, Phys. Rev. A 21, 2087 (1980).

[5] J. M. J. van Leeuwen, J. Groeneveld, and J. De Boer, Physica 25, 792 (1959).

[6] M. Baus and J. P. Hansen, Phys. Rep. 59, 1 (1980).

[7] H. E. DeWitt, Phys. Rev. A 14, 1290 (1976).

[8] J. P. Hansen, J. Phys. C (Paris) 41, 2 (1980).

[9] Y. Rosenfeld and N. W. Ashcroft, Phys. Rev. A 20, 1208 (1979).

[10] H. Iyetomi and S. Ichimaru, Phys. Rev. A 25, 2434 (1982).

[11] P. Hohenberg and W. Kohn, Phys. Rev. 136, B864 (1964); W. Kohn and L. J. Sham, *ibid.* 140, A1133 (1965).

[12] J. K. Percus, in *The Equilibrium Theory of Classical Fluids,* edited by H. L. Frisch and J. L. Lebowitz (Benjamin, New York, 1964), II-33.

[13] J. Chihara, Prog. Theor. Phys. 59, 76 (1978).

[14] S. Chakravarty and N. W. Ashcroft, Phys. Rev. B 18, 4588 (1978).

[15] H. Iyetomi (unpublished).

[16] C. Deutsch, Y. Furutani, and M. M. Gombert, Phys. Rev. A 13, 2244 (1976).

[17] F. Y. Wu and M. K. Chien, J. Math. Phys. 11, 1912 (1970); F. Y. Wu, J. Math. Phys. 12, 1923 (1971).

[18] E. E. Salpeter, Austr. J. Phys. 7, 373 (1954).

[19] We set $B(0)/B_{CK}(0)=1$ in the range of $\Gamma\lesssim 4$, where the estimated value $|B(0)|$ in the ion-sphere model is smaller than $|B_{CK}(0)|$. This simply points to a breakdown of the ion-sphere model in the weak coupling domain. One cannot take $f(r)=1$ in the range, $\Gamma>4$, simply because $B_{CK}(0)$ grossly underestimates the real $B(0)$. When the improved HNC calculations are carried out, nevertheless, by assuming $f(r)=1$, we find that the results amount to only a slight and insignificant improvement over the HNC results, both for the

radial distribution function and for the internal energy calculation. For example, the thermal fraction of the excess internal energy calculated by assuming $f(r)=1$ is 2.31 at $\Gamma=80$ and 2.91 at $\Gamma=160$; those are to be compared with the values listed in Table II.

[20]Q. N. Usmani, B. Friedman, and V. R. Pandharipande, Phys. Rev. B 25, 4502 (1982).

[21]K. C. Ng, J. Chem. Phys. 61, 2680 (1974).

[22]S. Galam and J. P. Hansen, Phys. Rev. A 14, 816 (1976).

[23]H. E. DeWitt, H. Graboske, and M. S. Cooper, Astrophys. J. 181, 439 (1973).

[24]N. Itoh, H. Totsuji, and S. Ichimaru, Astrophys. J. 218, 477 (1977).

[25]B. Jancovici, J. Stat. Phys. 17, 357 (1977).

[26]Since $c(r)$ rapidly approaches its Debye-Hückel limit $-\beta v(r)$ in the long-range domain beyond the first maximum of $g(r)$, it may be sufficient to compare the values of $c(r)$ at the origin between the MC and IHNC results.

[27]For example, see S. Ichimaru, *Basic Principles of Plasma Physics* (Benjamin, Reading, Mass., 1973), Chap. 2.

[28]J. A. Barker and J. J. Monaghan, J. Chem. Phys. 36, 2564 (1962); see also, A. D. J. Haymet and S. A. Rice, *ibid.* 74, 3033 (1981).